

Fabrication of polymer waveguides by laser ablation using a 355 nm wavelength Nd:YAG laser

^{1,2}Shefiu S. Zakariyah, ¹Paul P. Conway, ¹David A. Hutt, ³David R. Selviah, ³Kai Wang, ⁴Jeremy Rygate, ⁴Jonathan Calver, ⁴Witold Kandulski

¹Wolfson School of Mechanical and Manufacturing Engineering, Loughborough University, Loughborough, UK.

²Electronics Manufacturing Engineering Research Group, University of Greenwich, UK

³Department of Electronic and Electrical Engineering, University College London (UCL), London, UK.

⁴Stevenage Circuits Limited, Caxton Way, Stevenage, UK

Email: shefiuz@theiet.org, S.S.Zakariyah@lboro.ac.uk

Abstract -

The demand for optical waveguides integrated into Printed Circuit Boards (PCBs) is increasing as the limitations of copper interconnects are being reached. Optical polymer materials offer a good solution due to their relatively low cost and compatibility with traditional PCB manufacturing processes. Laser ablation is one method of manufacture, for which excimer lasers have been used, but UV Nd:YAG (Neodymium-doped Yttrium Aluminium Garnet) lasers are an attractive alternative due to their widespread use within the PCB industry for drilling vias. In this paper, 355nm, 60ns pulse length UV Nd:YAG laser ablation of Truemode™ acrylate-based optical polymer was investigated. The UV Nd:YAG laser was found to be able to ablate the polymer efficiently and the effects of laser ablation power and pulse repetition frequency (PRF) on depth of ablation were studied and used to determine optimum settings. Multimode optical waveguides were fabricated to demonstrate the process and optical loss measurements were carried out. These measurements demonstrated that the structures were able to transmit light at the data communications wavelength of 850 nm (NIR), but further work is required to reduce the level of loss. The use of UV Nd:YAG as a possible alternative to excimer for laser micromachining would facilitate the rapid deployment of the optical technology within the PCB industry.

Index -Laser ablation, Optical waveguides, UV Nd:YAG, Polymer, PCB, Interconnection, High bit rate, Optical circuit board, Optical backplane.

Introduction

High bit rate interconnections for long-haul communication is now an established technology with optical fibres (or waveguides) used to transmit signals. In recent years there has been ongoing research inclined towards adapting the same principles for use at the printed circuit board level driven by the requirements for higher data transfer rate, higher density interconnections and smaller package sizes amongst others, which have proven impracticable and uneconomic using conventional electrical connections [1 - 3]. The optical signal is guided along the waveguide by total internal reflection (TIR) as in optical fibres.

For this technology, polymer waveguides are favoured not only because of the ease of their fabrication and integration with other optoelectronic devices, but more importantly because of their compatibility with printed circuit board (PCB) manufacturing processes, e.g. lamination [4 -7].

A number of different methods of fabricating polymer optical

waveguides have been demonstrated in the literature including photolithography, wafer-level stack process and laser direct writing [6– 16]. Laser ablation offers an alternative approach. Figure 1 shows a schematic diagram of the three main stages involved in fabricating polymer waveguides by laser ablation in a single layer as considered in this paper. In the first stage, liquid optical polymer is spun on FR4 laminates and subsequently UV cured to form both the lower cladding and the core layers. Laser ablation is carried out in the second stage to machine channels/tracks such that a ridge of polymer is left in-between the channels to form the waveguide. For one or more adjacent waveguides, the number of grooves required is equal to $(n+1)$, where n is the number of adjacent waveguides. Finally, a layer of upper cladding is deposited using spin coating and then UV cured. For data communication applications low cost is essential and so multimode waveguides are preferred due to reduced cost of alignment of input and output optical components although recent research has shown how high alignment accuracy can be achieved at low cost [7].

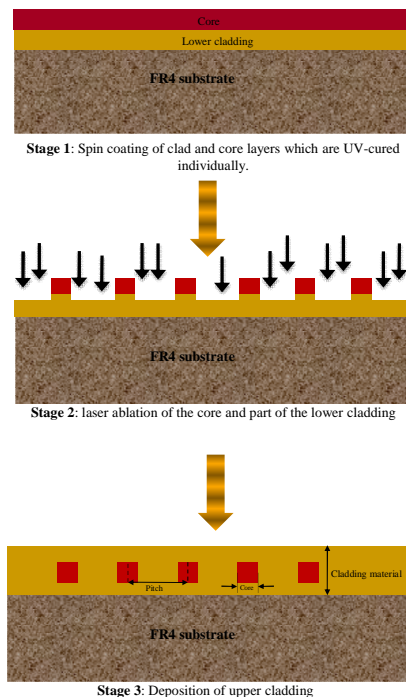


Figure 1: Schematic diagram (side view) of the three main stages in the fabrication of optical waveguides by laser ablation.

Laser ablation is commonly used to fabricate microvias for high density interconnects in the PCB manufacturing [18 - 21]. The initial use of the carbon dioxide (CO₂) lasers for laser micromachining offered a significant improvement, in terms of speed and quality, over traditional mechanical hole drilling. However, the width of the machined hole obtained with CO₂ is only in the range of 100 – 200 μm, which is becoming insufficient for current small-size high density multilayer PCB circuits for optoelectronic and photonic devices [20, 22]. In addition, copper which is used for the conducting tracks in current PCBs, reflects light of about 10 μm [18] wavelength, which is near the CO₂ laser wavelength of 10.6 μm making the CO₂ laser unsuitable for drilling through hole vias in multi-layer PCBs. These challenges have been overcome with the introduction of the Neodymium-doped Yttrium Aluminium Garnet (Nd:YAG) laser that offers, among other benefits, a smaller spot size and a wavelength or wavelengths ($\lambda = 10.64 \mu\text{m} - 213 \text{nm}$) [23, 24] that are readily absorbed by copper. However, Nd:YAG lasers have not yet completely replaced CO₂ lasers in the PCB industry. The CO₂ laser is the most suitable laser for blind hole via drilling as it terminates at the dielectric material-copper layer interface without causing damage to the copper pad [18].

Excimer laser ablation of optical polymers, typically at 193 nm (with ArF) and 248nm (with KrF), has been repeatedly reported in the literature [25-28]. In this technology, high quality micromachining, sometimes referred to as 'cold ablation', is thought to be due to the UV absorption and the short pulse time of the excimer laser. Therefore, since UV Nd:YAG (355 nm wavelength) lasers offer the same features, this paper investigates whether it could be adapted to perform a similar action. Little earlier research has been reported for their application for use in polymer waveguide fabrication except in [25, 29, 30] where waveguide fabrication of ORganic MODified CERamic (ORMOCER) was performed at 1 mm/s, for which both energy and pulse repetition frequency (PRF) were observed to have an impact on the smoothness of the waveguide side wall which is crucial to minimise propagation loss, but further optimization was required. Steenberge, et. al. [29] noted that both photothermal and photochemical processes were present during the fabrication, due to the higher wavelength (355 nm) of the UV Nd:YAG compared to the KrF excimer laser; although, waveguide loss measurements were not yet reported and the values of wall roughness were not stated. The first measurements of side wall roughness of polymer waveguides have only been reported recently [31]. Therefore, this paper investigates the use of UV Nd:YAG lasers and the optimisation of the fabrication process using another polymer popularly used for optical waveguides due to its inherently low loss for use in Optical Interconnects (OI).

Experimental design and measurement

The UV Nd:YAG laser used in this work was a diode-pumped frequency-tripled UV Nd:YAG laser system manufactured by Electro Scientific Industries (ESI) model 5200 UV μVia Drill, which is hosted by Stevenage Circuits Limited. This operates at a wavelength of 355nm (i.e. near ultraviolet) with 60 ns pulse-width, and with laser ablation power and pulse repetition frequency (PRF) of up to 3 Watts and 20 kHz respectively. The beam intensity profile was Gaussian with a fixed beam

diameter of 25 μm at the full width half maximum. Therefore, machining a groove of dimensions greater than 25 μm wide required the beam passes to be overlapped. Experiments were conducted to determine the effects of laser ablation power and PRF on the machining of grooves. Depth measurements of the features (ablated tracks and waveguides) were carried out after a cleaning process was undertaken and upper cladding had been applied where applicable. For this, the samples were diced, mounted and polished such that the depth measurement could be obtained by looking at the cross-section profiles of the ablated structures using a Flash™200 optical measuring device.

Sample preparation and fabrication

In this research, Truemode™ photopolymer provided by Exxelis Ltd, Edinburgh, UK was used. It is a UV-curable mixture of acrylate and methacrylate monomers that is liquid at room temperature. The fact that its absorption loss is very low with a typical value of < 0.04 dB/cm @ 850 nm wavelength and that it can withstand conventional PCB fabrication, i.e. high pressure lamination and high temperature solder reflow processes, makes it a suitable choice for OI [32]. There are various formulations of this polymer available from the supplier. For the work reported in this paper, EXX-clad 277 and EXX-core 37E formulations were used having refractive indices of 1.5265 and 1.5560 respectively at 850 nm.

The stages or processes involved in laser ablation of a polymer waveguide as employed in this research are shown in figure 2. Single layer waveguide fabrication was the focus of this research, as this is currently enough to provide the bandwidth density requirements for OI; future work could extend these processes to multiple layers of waveguides such as those considered in [27]. Prior to polymer deposition, FR4 samples were normally cleaned in methanol to remove micro-particles from the substrate surface; the samples were then dried in an oven at 80 °C – 100 °C for about 1 min to ensure they were moisture-free. Due to possible debris deposition on the ablated structures and other forms of contamination, samples were also cleaned using either methanol or iso-propanol, before depositing the upper cladding and also during sampling and polishing of mounted sample(s). In the case of serious contamination which could be observed visually, and sometimes, with the aid of an optical microscope, ultrasonic agitation (sonication) was additionally required. This was achieved by putting the sample(s) in a beaker containing methanol or iso-propanol which was then immersed in an ultrasonic bath. The sonication period varied from a minute to three minutes, depending on the nature or amount of debris to be removed.

The layers of optical polymer were deposited by spin coating usually at 350 – 450 rpm for 30 seconds to obtain 30 – 50 microns thickness, typical of that required for a multimode waveguide core; dimensions such as 20 μm × 20 μm, 35 μm × 35 μm, 50 μm × 50 μm, 85 μm × 100 μm have been reported [5,29,33]. The lower cladding and core layers were deposited sequentially, with the lower cladding layer cured before deposition of the core layer. Curing of the polymers was carried out by exposure to UV light for 3 – 4 minutes in an oxygen free nitrogen atmosphere to cross-link the polymer and finally oven-baked at 100°C for 60 minutes. Thicker

layers were prepared using multiple deposition cycles.

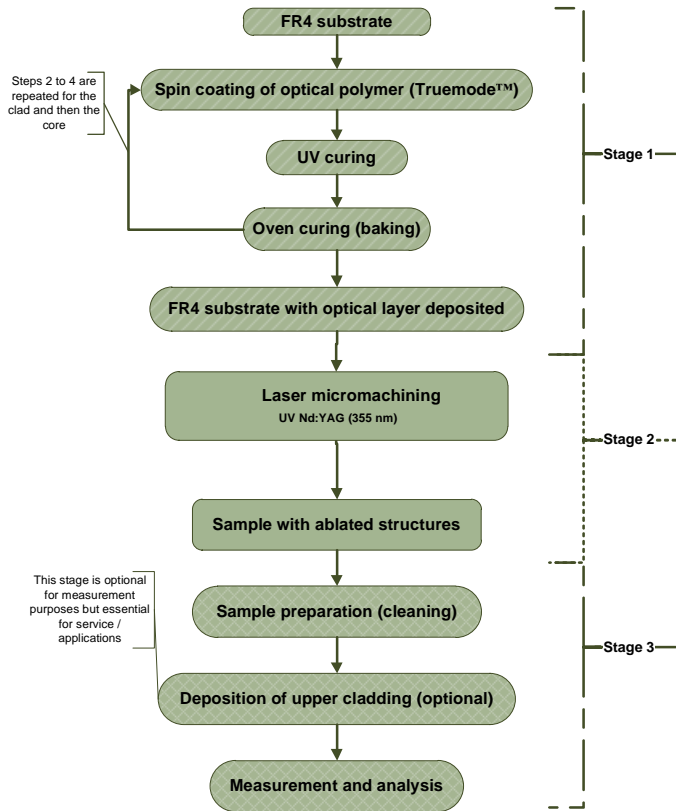


Figure 2: Flow diagram of the processes involved in patterning optical polymer waveguides using laser ablation.

Feasibility study - initial laser machining

The initial trial was largely focused on the laser-material interaction with particular emphasis on the laser beam absorption and the possibility of using this class of laser to process Truemode™ acrylate based photopolymer. A similar laser has been reportedly used for ablating other polymers [18, 20, 34]. A first micromachining trial was conducted with the UV Nd:YAG laser using the host (Stevenage Circuits Ltd, UK) parameter settings suitable for processing PCB materials. The results showed poor machining of the Truemode™ polyacrylate material which were thought to be due to incorrect selection of parameters; further trials were however carried out with emphasis on optimising the process. Following the trials, the authors observed: (i) that the Truemode™ polyacrylate photopolymer absorbs at the UV Nd:YAG wavelength of 355 nm, (ii) that laser ablation power and PRF are salient factors that affect the depth of ablation and thus require further investigation, and (iii) that ablation at relatively high speed above 30 mm/s is not suitable and similarly, relatively high laser ablation power above 0.3 Watt is too thermally-damaging for the material. This formed the basis of the choice of the 'operating window' used during the subsequent laser characterisation.

Laser system characterisation

The effects of the laser ablation power and PRF on the depth of ablation were studied. In each case, all factors were kept

constant with the exception of the one under investigation and used to ablate 75 µm wide, 50 mm long channels.

1.

Laser Ablation Power

In this experiment, all factors were fixed while laser ablation power was increased at an interval of 0.05 Watt from 0.1 Watt to 0.25 Watt. Figures 3 and 4 show optical microscope images of the cross-section and plan views respectively of the four different channels machined at 0.1 Watt, 0.15 Watt, 0.2 Watt and 0.25 Watt in input laser ablation power. It is obvious from the cross-sectional view of the ablated structures shown in figure 3 that an increase in laser ablation power resulted in an increase in the amount of material removed with minimum and maximum etch achieved at 0.1 Watt (figure 3a) and 0.25 Watt (figure 3d) respectively. The ablated channels at these settings (with laser ablation power varying) produced straight edges as shown in figure 4. Figure 4 also show that the width of the ablated groove increases with an increase in laser ablation power, which might be due to a thermal effect as the laser ablation power density increases. It is observed that the structures are tapered; this tapering effect can be due to a number of factors such as the beam profile (Gaussian in this case), beam shape, which is circular, and incident light diffraction [26,35]. The figures also show some black carbonised debris remaining in the bottom of the hole in figure 3(b), (c) and (d).

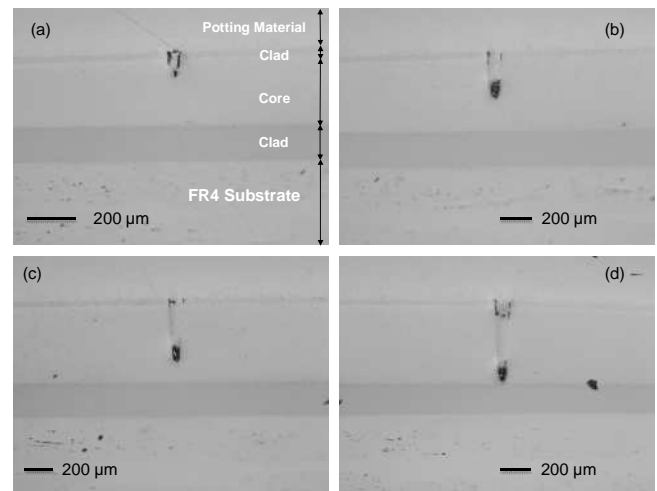


Figure 3: Cross-section of structures machined in Truemode™ polyacrylate optical polymer at 10 kHz, 10 mm/s, 75 µm linewidth and six passes but varying input laser ablation power (a) 0.1 Watt, (b) 0.15 Watt, (c) 0.2 Watt, and (d) 0.25 Watt.

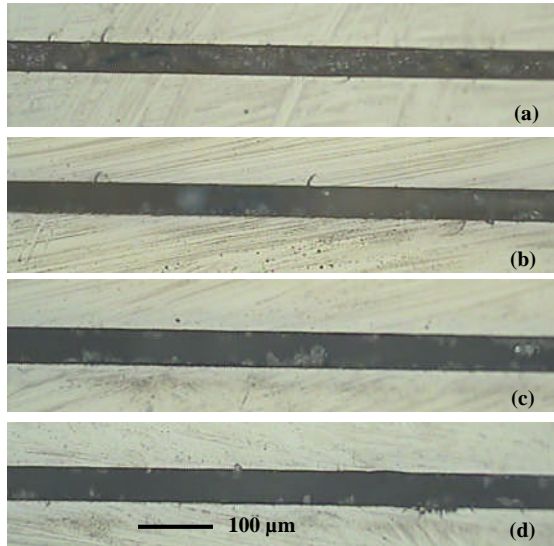


Figure 4: Plan view of structures machined in Truemode™ polyacrylate optical polymer at 10 kHz, 10 mm/s, 75 μm linewidth and six passes, but varying input laser ablation power (a) 0.1 Watt, (b) 0.15 Watt, (c) 0.2 Watt, and (d) 0.25 Watt.

The graph shown in figure 5 is a plot of the relationship between the input laser ablation power and the depth of ablation which indicates a direct relationship between the two factors. The ablation (power) threshold at 10 kHz and 10 mm/s is obtained by extrapolating the graph in figure 5, which is ~0.08 Watt. The estimated threshold here suggests that the ablation of Truemode™ polyacrylate using this system ought to be carried out at a value greater than 0.08 Watt, however, the operating laser ablation power should be maintained only a little above the laser ablation power threshold, e.g. 0.1 Watt - 0.2 Watt, to avoid the dominance of photothermal over photochemical processes. This data further supports the observation made during the initial trials where ablating at high laser ablation power produced poor results.

A curve fitting (represented by the dotted line in figure 5) provided a mathematical means of representing/interpreting the behaviour of the process as shown in equation 1, where D is the depth of ablation in microns and p , the input laser ablation power in Watts. A similar graph showing the relationship between the laser ablation power and the depth of ablation is plotted in figure 6 with the x-axis representing the ratio of the input laser ablation power to the estimated laser ablation power threshold denoted as p and p_i , respectively. The ablation power threshold, p_i , used is that obtained earlier (from figure 5) of 0.08 Watt. The resulting equations 1 and 2 are similar with each having an R^2 of 0.9982 and the coefficient of the logarithmic term in both equations is also equal with a value of 488.54.

R -squared (R^2) is a measure of correlation of data having a minimum and maximum value of 0 and 1 respectively; the closer this value is to unity, the better the relationship between two variables. The fact that the R^2 values obtained for equations 1 and 2 are very close to unity suggest that logarithmic equations fit well to the laser-material interaction at this wavelength. It is worthwhile mentioning at this point that an attempt was made to fit the curve with other 'models' such as linear and exponential models, but the R^2 values obtained were lower than that of a logarithmic function; for example, the R^2 for linear and exponential fittings were

0.9889 and 0.9641 respectively. Although, these values also showed a high degree of correlation, nevertheless, the logarithmic function still offered a better degree of confidence. Furthermore, the two commonly cited 'models' for laser material processing, namely, Beer's law and Srinivasan-Smrtic-Babu (SSB)'s model, are also based on a natural logarithmic relationship [36].

As previously mentioned, Steenberge et. al [29] observed that due to the high wavelength of UV Nd:YAG compared to excimer lasers, the photothermal process cannot be ignored for ablation (of ORMOCER) at this wavelength. Winco et. al also concluded in [21] that due to an apparent melting effect during the ablation of polyimide at 355 nm, the mechanism has a photothermal contribution. The regression lines (equations 1 and 2) plotted on the graph of the relationship between the laser ablation power and depth of ablation have two terms/parts. This is similar in form to Srinivasan-Smrtic-Babu (SSB)'s mathematical representation [36] of the laser ablation process with two terms each representing photothermal and photochemical contributions. Therefore, the authors favour the complementary effect of photochemical and photothermal mechanisms for the laser ablation of Truemode™ photopolymer at 355 nm wavelength using UV Nd:YAG laser.

$$= 488.54 \ln(p) + 1214.8 \quad (1)$$

$$= 488.54 \ln(p/p_i) - 19.102 \quad (2)$$

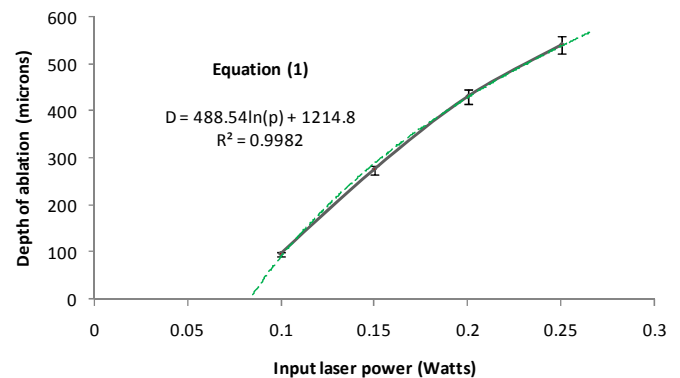


Figure 5: The depth of ablation plotted versus the input laser ablation power at 10 mm/s translation speed 10 kHz after scanning six times. .

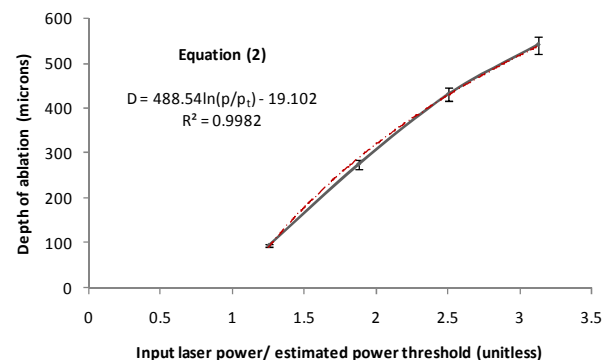


Figure 6: The depth of ablation plotted versus the ratio of (input laser ablation power / estimated laser ablation power threshold) at 10 mm/s translation speed, 10 kHz after six scans. .

2.

ulse repetition frequency (PRF)

Reports have indicated different behaviours, depending on the laser wavelength and material absorption, with regards to the effect of the pulse repetition rate/frequency (PRR/PRF) on the depth of ablation. To investigate the relevance of PRF, all other experimental parameters: laser ablation power, translation stage speed and number of scans were kept constant at 0.1 Watt, 5 mm/s and 4 passes respectively with the exception of PRF, which was increased at intervals of 5 kHz between 5 kHz and 20 kHz.

Figure 7 shows the cross-section of the four different channels ablated by changing the PRF, while figure 8 is the plan view of the same set of channels. The plot of PRF against the depth of ablation is shown in figure 9; this indicates a decrease in ablation depth from 5 kHz to 15 kHz, thereafter, a steeper increase is noticed from 15 kHz to 20 kHz.

In the first three instances, i.e. from 5 kHz to 15 kHz, where there was a decrease in the depth of ablation as the PRF increased, it could be argued that the depth decrease was due to the fact that though more pulses per area were released per second at higher frequencies, the energy per pulse was reduced. This is because, since the average laser ablation power of the laser remained constant at 0.1 Watt, the energy per pulse, which is equal to the average laser ablation power divided by the PRF, decreased. In other words, both the PRF and energy per pulse played their individual role at this instance. A sudden rise in the depth of ablation at 20 kHz, which has the least pulse energy, can only be explained if the ablation at 355 nm is considered to be both photochemical and photothermal [29,34]. While the former is a function of pulse energy and ablation threshold, the latter is related to an effective frequency factor, activation energy and temperature [36]. In other words, the ablation caused by a photothermal process is largely independent of the pulse energy, but rather depends on the thermal energy at the ablation zone, which increases for example when excess pulses are used at high PRF.

Furthermore, it could be that PRF has no direct effect on the quantity of ablation within this PRF range as some authors have reported [37] for excimer laser ablation of polymers with high absorption coefficients, namely: polycarbonate (PC), polyethylene terephthalate (PET), polyimide (PI) and polystyrene (PS). It is also possible that specific PRF perform optimally at particular combinations with other parameters. In other words, the effect of PRF is determined and influenced by a combination of other factors.

In addition to debris in the bottom of the hole in figure 7, a black spot is observed at the lower cladding-FR4 region (figure 7d), which is probably caused by laser light transmitted down to the next interface between material causing a localised heating.

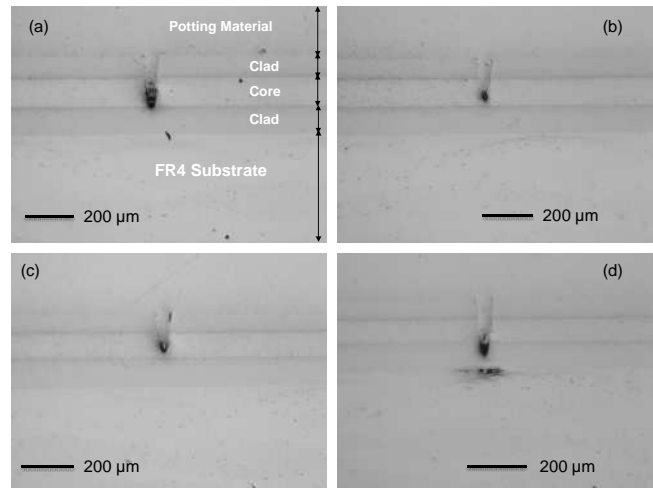


Figure 7: Cross-section of structures machined in Truemode™ optical polymer at 0.1 Watt, 5 mm/s and four passes but varying PRF: (a) 5 kHz, (b) 10 kHz, (c) 15 kHz, and (d) 20 kHz.

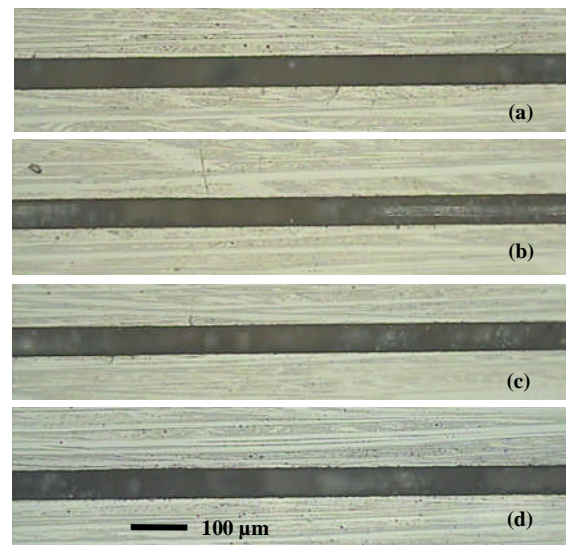


Figure 8: Plan view of structures machined in Truemode™ optical polymer at 0.1 W, 5 mm/s and four passes but varying PRF (a) 5 kHz, (b) 10 kHz, (c) 15 kHz, and (d) 20 kHz.

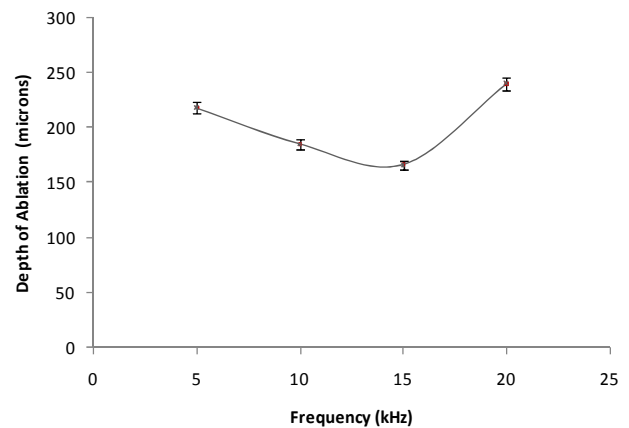


Figure 9: Depth of ablation plotted versus the pulse repetition frequency of the laser at a constant laser ablation power of 0.1 Watt, a translational stage speed of 5 mm/s and after four scans.

UV Nd:YAG polymer waveguide fabrication

Since a single guide was employed in all instances of the fabrication process, two grooves were machined with the spacing between the two equal to the width of the intended waveguide. As shown earlier in figure 1, the depth of the grooves went beyond the core layer into the lower cladding. Once the fabrication exercise was accomplished, the samples were then analysed mainly to detect the presence of a ‘continuous’ waveguide prior to loss measurement; this was achieved by passing light (from a Flash™200 optical measuring device) into one end of the guide for possible detection at the other end, i.e. backlighting, and this was used to determine the waveguide dimension. Figure 10 shows the image of a single multimode waveguide of $45\ \mu\text{m} \times 45\ \mu\text{m}$ and 60 mm long illuminated from behind using the Flash™200 system; the structure was made by ablating $\sim 200\ \mu\text{m}$ wide grooves in Truemode™ polyacrylate.

Having demonstrated the viability of polymer waveguide fabrication, subsequent experiments were centred on studying the effects of the laser system variables on the optical transmission loss of the waveguides. That is to say, the research aimed to fabricate waveguides with one variable changing while other factors were fixed in order to understand how this variable contributed to the propagation loss. The propagation loss measurements for the waveguides were carried out at University College London (UCL), using an input multimode (MM) Vertical Cavity Surface Emitting Laser (VCSEL) at nominally 850 nm wavelength (depending on its temperature) as the input light source which was coupled to a 10 m 50/125 step index multimode fibre for launching light into the waveguides. The optical fibre was wound around a cylinder to fully fill the modes and this was checked to confirm that they had been fully filled. An integrating sphere photo detector (PD) was used to monitor the output laser ablation power emerging from the waveguide channel and a $70\ \mu\text{m}$ circular pin-hole was placed in front of the integrating sphere to filter out most of the light passing through the cladding. Both the integrating sphere photodetector and the light launching fibre were mounted on 3-axis motorized translation stages for alignment to the waveguide. This measurement method gives the total insertion loss (equation 3) where, IL , PL , L and CL are the Insertion loss, Propagation loss, Waveguide length and combined input and output Coupling loss respectively. Reference[38] indicates how the various components of the total loss can be established.

$$= \quad + \quad (3)$$

However, since the “cut-back” method was not employed in this measurement, the loss reported here for the samples are the total waveguide loss. Therefore, propagation losses were calculated based on the coupling loss obtained from other measurements carried out on the same system which was ~ 4.5 dB.

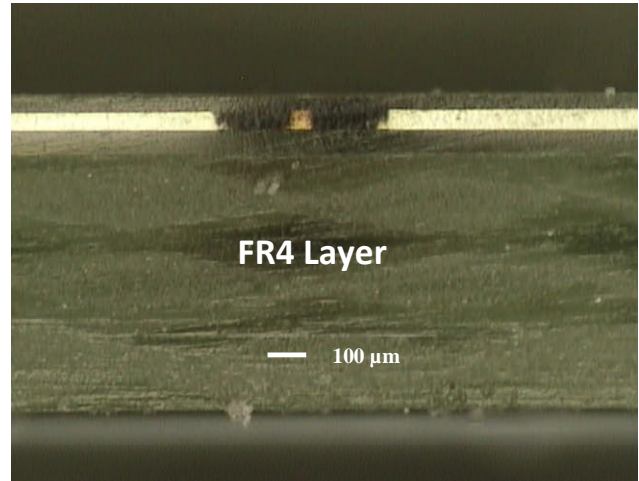


Figure 10: Waveguide of $45\ \mu\text{m} \times 45\ \mu\text{m}$ made in Truemode™ polyacrylate using the 5200 model UV Nd:YAG laser system at 5 mm/s, 5 kHz, 0.1 Watt after a single pass.

For the purpose of loss measurement, the effect of varying the laser ablation power and PRF from 0.11 Watt to 0.13 Watt and 8 kHz to 12 kHz respectively were considered while keeping the translation speed and number of passes constant at 5 mm/s and 1 scan in all cases. Additionally, an ablated channel of $\sim 200\ \mu\text{m}$ wide was used for all the samples with a spacing of $50\ \mu\text{m}$ left between the channels to represent the waveguides. The parameters were chosen following the laser system characterisation results presented above; for example, the PRF was kept within the range 5 kHz – 15 kHz, where its relationship with the depth of ablation was close to linear. The input laser ablation power and translation speed were maintained at the minimum possible values, i.e. below 0.15 Watt and 5 mm/s respectively, as this was found to give better quality ablation. The minimum input laser ablation power helped in reducing the thermal damage that could result from the photothermal contribution to the process while the low scanning speed ensured optimum pulse overlap and smooth edge finish.

With varying laser ablation power, the PRF, translation stage speed and number of passes were kept fixed at 5 kHz, 5 mm/s and 1 scan respectively; while with varying PRF, input laser ablation power was maintained at 0.12 Watt and the number of passes and the speed of the translation were both fixed at 5 mm/s and 1 scan. In all cases, the length of the fabricated waveguides were 40 mm. Figure 11a is the plot of PRF against insertion loss and figure 11b is the plot of laser ablation power against the insertion loss.

In figure 11a, for an increase in PRF from 8 kHz to 12 kHz there appears to be a slight decrease in the insertion loss of the waveguide. A possible explanation of this effect is that, at high PRF, the stability and intensity distribution of the laser beam was improved. As a result of this improvement in the beam quality, the ablated profile became better. In addition, since the energy per pulse at constant average laser ablation power decreases as the PRF increases, it thus follows that the decrease in the insertion loss in this case corresponds to lowering the pulse energy used during the ablation process. This means that, for the range of parameters considered, the minimum insertion loss was achieved at 0.01 mJ/pulse obtained by dividing the input laser ablation power with

operating PRF, i.e. 0.12 /

Figure 11b shows that an increase in laser input power caused a corresponding increase in the insertion loss over the range of values considered. This relationship between the laser ablation power and loss could be due to the thermal damage that might have been caused by the excess laser ablation power. In addition, it could be argued that the excess laser ablation power input caused some changes in the material characteristics such as refractive index [39,40] which might affect the containment of light in the core by TIR thus contributing to the optical loss along the waveguide channel.

In figure 11c, a plot of insertion loss versus the energy per pulse is presented; the pulse energies used in this case were those calculated from figures 11a and 11b assuming the fact that energy/pulse (mJ) is equal to input laser ablation power (Watt) divided by the PRF (kHz) as previously asserted. Due to the high loss value obtained for the 0.015 mJ/pulse it is difficult to draw clear conclusions from the data, however depending on the significance of this data point, it would seem that lower pulse energies produced waveguides with lower insertion loss.

In this study, the minimum insertion loss was 10.2 dB obtained independently at (i) 5mm/s, 5 kHz and 0.11 Watt, and (ii) 5 mm/s, 12 kHz and 0.12 Watt. The combined input and output coupling loss was measured to be 4.5 ± 0.5 dB on a similar waveguide sample. If we assume that the coupling loss is at the same level in this case, then the propagation loss of the laser ablated waveguide is 1.4 ± 0.5 dB/cm. This is quite promising considering the range quoted in the literature [20, 41, 42] coupled with the fact that there was no precedence (for this class of laser) upon which a benchmark could be set.

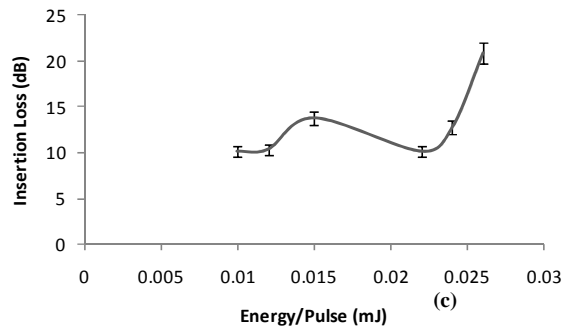
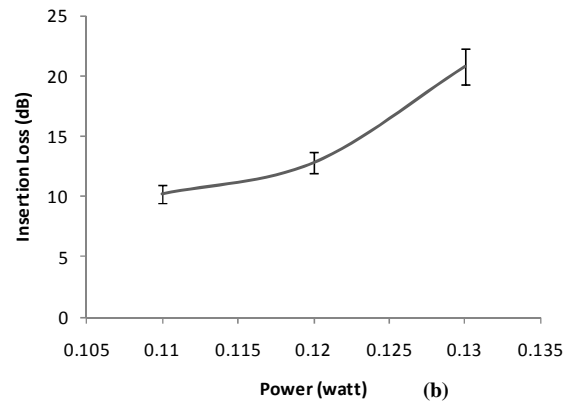
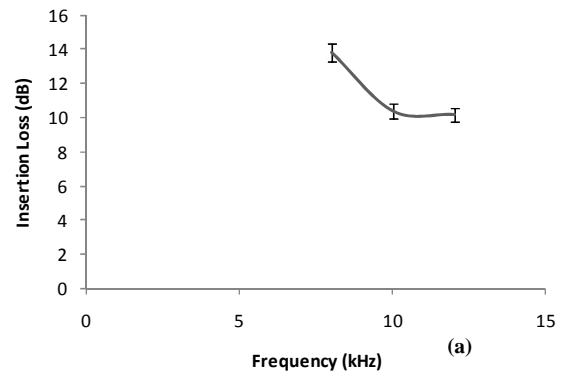


Figure 11: Optical loss measurement carried out on samples from UV Nd:YAG showing the relationships between (a) PRF and insertion loss, (b) input laser ablation power and insertion loss, and (c) calculated pulse energy and insertion loss.

Conclusion

A 355 nm diode-pumped third harmonic UV Nd:YAG laser within an ESI 5200 UV μ Via Drill (hosted by Stevenage Circuits Limited, UK) was used to machine structures in Truemode™ photopolymer. Its pulsed mode, short wavelength in the UV region and pulse duration of 60 ns are some of the key benefits of this laser, which the authors believe can allow it to complement and/or act as an alternative to the excimer laser for the application under investigation. Based on initial trial results and further systematic studies to measure the depth of ablation as a function of laser system parameters an optimum operating window for polymer waveguide fabrication was identified and believed to be at 0.1 ± 0.02 W,

10 ± 2 kHz and 5 – 10 mm/s.

Effects of laser ablation power (0.1 Watt to 0.25 Watt), PRF (5 kHz to 20 kHz) on the depth of ablation were studied. While the graph of the relationship between the laser ablation power and depth of ablation indicates a logarithmic increase in the depth as the laser ablation power increased as expected and in line with literature reports, the relationship between the change in PRF and the depth of ablation showed some anomalies. Although this is not uncommon, the authors believe that this effect supports the presence of both photothermal and photochemical mechanisms for ablation at this wavelength.

Optical waveguides were fabricated and loss measurements carried out to investigate the effects of different machining parameters. A minimum insertion loss of 10.2 dB (including propagation loss and coupling loss) was obtained for 40 mm long waveguides corresponding to a propagation loss of 1.4 ± 0.5 dB/cm. This study on UV Nd:YAG laser ablation of polymer waveguides indicates the potential for this as a low-cost production route since the laser is currently used for high volume PCB production, however, further loss reduction should be considered in the future.

Acknowledgments

The research was part of the Integrated Optical and Electronic Interconnect PCB Manufacturing (OPCB) IeMRC Flagship Project, financially supported by the UK Engineering and Physical Sciences Research Council, EPSRC, through the Innovative Electronics Manufacturing Research Centre (IeMRC) and by the 8 collaborating companies in the OPCB project. The authors particularly thank Exxel Ltd for providing the optical polymers used. The authors also thank the 3 collaborating universities in the consortium. The authors wish to thank Khadijah Olaniyan and Richard Pitwon for helpful discussions.

References

1. pitwon, R.C.A., Hopkins, K., Wang, K., Selviah, D.R., Baghsiahi, H., Offrein, B.J., Dangel, R., Horst, F., Halter, M. and Gmür, M. (Invited Paper) [7607-18], "Design and implementation of an electro-optical backplane with pluggable in-plane connectors", Proceedings of SPIE (7607), International Society for Optical Engineering, Bellingham, WA, USA (2010).
2. lebov, A. L., Lee, M. G. and Yokouchi, K. Integration technologies for pluggable backplane optical interconnect systems. *Optical engineering: the journal of the Society of Photo-optical Instrumentation Engineers*. 46, 15403 (2007).
3. hn, S., Cho, I., Han, S., Byoung Yoon, K. and Lee, M. Demonstration of high-speed transmission through waveguide-embedded optical backplane. *Optical engineering: the journal of the Society of Photo-optical Instrumentation Engineers*. 45, 85401 (2006).
4. ang, K. and Selviah, D.R. and Papakonstantinou, I. and Yu, G. and Baghsiahi, H. and Fernández, F.A. (2008) Photolithographically manufactured acrylate multimode optical waveguide loss design rules. 2nd Electronics System-Integration Technology Conference, ESTC 2008, Greenwich, London, UK, VOLS 1 AND 2, PROCEEDINGS, 1251-1255 (2008)
5. angel, R. et al. Development of a low-cost low-loss polymer waveguide technology for parallel optical interconnect applications. *Biophotonics/Optical Interconnects and VLSI Photonics/WBM Microcavities, 2004 Digest of the LEOS Summer Topical Meetings*, 2 pp. (2004).
6. oon, K. B. et al. Optical backplane system using waveguide-embedded PCBs and optical slots. *J. Lightwave Technol.* 22, 2119-2127 (2004).
7. aeda, Y. et al. Polysiloxane based optical waveguide equipped with fibre guides by using direct photolithography technique. 1 (2005).
8. uyal H, Waddie AJ, Mackintosh AR, et al. "Light emitting polymer blends and diffractive optical elements in high-speed direct laser writing of microstructures" *JOURNAL OF PHYSICS D-APPLIED PHYSICS* Volume: 41 Issue: 9 Article Number: 094009 (2008).
9. lebov, A. L., Yokouchi, K., Roman, J. and Lee, M. G. Optical interconnect modules with fully integrated reflector mirrors. *IEEE Photonics Technology Letters* 17, 1540-1542 (2005).
10. opetz, S., Rabe, E., Kang, W. and Neyer, A. Polysiloxane optical waveguide layer integrated in printed circuit board. *Electron. Lett.* 40, 668-669 (2004).
11. nakenborg, D., Perozziello, G., Klank, H., Geschke, O. and Kutter, J. Direct milling and casting of polymer-based optical waveguides for improved transparency in the visible range. *J Micromech Microengineering* 16, 375-381 (2006).
12. . Ponoth, Peter D. Persans, Ram Ghoshal, N. Agarwal, Joel L. Plawsky, A. Filin, and Q. Z. Fang. Siloxane-based polymer epoxies for optical waveguides. In *Proceedings of SPIE Applications of Photonic Technology 6*, volume 5260, pages 331–335, 2003.
13. erm, Paul M. and Lawrence W. Shackjette, High Volume Manufacturing of Polymer Waveguides via UV-Embossing, *SPIE*, Vol. 4106, 1-10, 2000.
14. akariyah, S. S. et al. *Polymer optical waveguide fabrication using laser ablation* *Electronics Packaging Technology Conference, 2009. EPTC '09*. 11th, 2009, pp. 936-941
15. iramatsu, S. & Kinoshita, M. Three-dimensional waveguide arrays for coupling between fiber-optic connectors and surface-mounted optoelectronic devices. *Lightwave Technology, Journal of* 23, 2733-2739 (2005).
16. elviah, D. R. et al. Integrated optical and electronic interconnect PCB manufacturing research. *Circuit World [Circuit World]*. Vol. 36 36, 5-19 (2010).
17. apakonstantinou, I., Selviah, D. R., Pitwon, R. & Milward, D. Low-Cost, Precision, Self-Alignment Technique for Coupling Laser and Photodiode Arrays to Polymer Waveguide Arrays on Multilayer PCBs. *Advanced Packaging, IEEE Transactions on* 31, 502-511 (2008).
18. ower, M. C. Industrial applications of laser micromachining. *Optics Express* 7, 56-67 (2000).
19. ung, K. C., Zeng, D. W. & Yue, T. M. XPS investigation of Upilex-S polyimide ablated by 355 nm Nd:YAG laser irradiation. *Appl. Surf. Sci.* 173, 193-202 (2001).
20. olden, H. T. The developing technologies of integrated optical

- waveguides in printed circuits. *Circuit World* 29, 42-50+9 (2003).
21. inco K.C. Yung, J.S. Liu, H.C. Man. Experimental investigation of 355nm Nd:YAG laser ablation of RCC in PCB. *Circuit World* 25, 13 -17 (1999).
 22. i, J. & Ananthasuresh, G. K. A quality study on the Excimer laser micromachining of electro-thermal-compliant micro devices. *Journal of micromechanics and micro engineering: structures, devices, and systems*. 11, 38-47 (2001).
 23. on, J. C. in *Laser processing of engineering materials: principles, procedure and industrial application 556* (Elsevier Butterworth-Heinemann, Oxford, 2005).
 24. teen, W. M. in *Laser material processing* (Springer, London, 2003).
 25. an Steenberge, G., Geerinck, P., Van Put, S. & Van Daele, P. Integration of multimode waveguides and micromirror couplers in printed circuit boards using laser ablation. *Proceedings of the SPIE - The International Society for Optical Engineering* 5454, 75-84 (2004).
 26. arvey, E. C., Remnant, J. L., Rumsby, P. T. & Gower, M. C. Microstructuring by Excimer laser. *Proc SPIE Int Soc Opt Eng* 2639, 266-277 (1995).
 27. endrickx, N. et al. Laser ablation as enabling technology for the structuring of optical multilayer structures. *Journal of Physics: Conference Series* 59, 118-21 (2007).
 28. homas, D.W., Foulkes-Williams, C., Rumsby, P.T., & Gower, M.C. Surface modification of polymers and ceramics induced Excimer laser radiation, in *Laser Ablation of Electronics Materials, Basic Mechanisms and Applications*, 1992.
 29. an Steenberge, G. et al. MT-compatible laser-ablated interconnections for optical printed circuit boards. *J. Lightwave Technol.* 22, 2083-90 (2004).
 30. an Steenberge, G ; Hendrickx, N ; Geerinck, P ; Bosman, E ; Van Put, S ; Van Daele, P; Development of a technology for fabricating low cost parallel optical interconnects.; *Proceedings of SPIE Photonics Europe Conference 2006 - 2006 - (Vol. 6185) p. 618507-1-618507-8*
 31. Papakonstantinou, I., James, R. & Selviah, D. R. Radiation- and Bound-Mode Propagation in Rectangular, Multimode Dielectric, Channel Waveguides With Sidewall Roughness. *Lightwave Technology, Journal of* 27, 4151-4163 (2009).
 32. Material Data Sheet [Accessed April 2011] : Available from : <http://www.exxelis.com/products/Truemode-datasheet-f.pdf>
 33. Immonen, M., Karppinen, M. and Kivilahti, J. K. Fabrication and characterization of polymer optical waveguides with integrated micromirrors for three-dimensional board-level optical interconnects. *Electronics Packaging Manufacturing, IEEE Transactions on* 28, 304-311 (2005).
 34. Yung, W.K.C., Liu, J.S., Man, H.C., Yue, T.M., 355 nm Nd:YAG laser ablation of polyimide and its thermal effect. *Journal of Materials Processing Technology* 101 (2000).
 35. akariyah, S.S. "Laser Ablation of Polymer Waveguide and Embedded Mirror for Optically-Enabled Printed Circuit Boards (OEPCB), PhD Thesis (2010), Loughborough University, UK.
 36. hin, B. S., Oh, J. Y. and Sohn, H. Theoretical and experimental investigations into laser ablation of polyimide and copper films with 355-nm Nd:YVO4 laser. *J. Mater. Process. Technol.* 187-188, 260-263 (2007).
 37. lly, E. K., Piper, J. A., Brown, D. J. W. & Withford, M. J. Enhanced polymer ablation rates using high-repetition-rate ultraviolet lasers. *IEEE Journal on Selected Topics in Quantum Electronics* 5, 1543-1548 (1999).
 38. apakonstantinou, I., Selviah, D. R. & Kai Wang. Insertion Loss and Misalignment Tolerance in Multimode Tapered Waveguide Bends. *Photonics Technology Letters, IEEE* 20, 1000-1002 (2008).
 39. reanton, V., et al. Engineering of waveguides and other microstructures in dielectrics. *Proceedings of the SPIE, Photonics North 2006, Vol. 6343, 634312*(2006).
 40. zcan, L. C. Fabrication of buried waveguides in planar silica films using a direct CW laser writing technique. *Journal of non-crystalline solids*. 354, 4833 (2008).
 41. eck, G. L. *et al.* Demonstration of direct coupled optical/electrical circuit board. *IEEE Transactions on Advanced Packaging* 32, 509-16 (2009).
 42. ldada, L. Polymer integrated optics: Promise vs. practicality. *Proc SPIE Int Soc Opt Eng* 4642, 11-22 (2002).

H

H

T

V

V

Z

S

I